



<b>Title</b>	<b>Scaling of three-dimensional InN islands grown on GaN(0001) by molecular-beam epitaxy</b>
<b>Author(s)</b>	<b>Cao, YG; Xie, MH; Liu, Y; Xu, SH; Ng, YF; Wu, HS; Tong, SY</b>
<b>Citation</b>	<b>Physical Review B - Condensed Matter And Materials Physics, 2003, v. 68 n. 16, p. 1613041-1613044</b>
<b>Issued Date</b>	<b>2003</b>
<b>URL</b>	<b><a href="http://hdl.handle.net/10722/43404">http://hdl.handle.net/10722/43404</a></b>
<b>Rights</b>	<b>Physical Review B (Condensed Matter and Materials Physics). Copyright © American Physical Society.</b>

## Scaling of three-dimensional InN islands grown on GaN(0001) by molecular-beam epitaxy

Y. G. Cao,<sup>1,2</sup> M. H. Xie,<sup>1,\*</sup> Y. Liu,<sup>1</sup> S. H. Xu,<sup>1</sup> Y. F. Ng,<sup>1</sup> H. S. Wu,<sup>1</sup> and S. Y. Tong<sup>3</sup>

<sup>1</sup>*Department of Physics and HKU-CAS Joint Laboratory on New Materials, The University of Hong Kong, Pokfulam Road, Hong Kong, China*

<sup>2</sup>*Institute of Physics, Chinese Academy of Sciences, Beijing 100080, China*

<sup>3</sup>*Department of Physics and Materials Science, City University of Hong Kong, Tat Chee Avenue, Kowloon, Hong Kong*

(Received 30 July 2003; published 13 October 2003)

The scaling property of three-dimensional InN islands nucleated on GaN(0001) surface during molecular-beam epitaxy (MBE) is investigated. Due to the large lattice mismatch between InN and GaN ( $\sim 10\%$ ), the islands formed from the Stranski-Krastanow growth mode are dislocated. Despite the variations in (residual) strain and the shape, both the island size and pair separation distributions show the scaling behavior. Further, the size distribution resembles that for submonolayer *homoepitaxy* with the critical island size  $i = 1$ , suggesting that detachment of atoms is not significant. The above results also indicate strain is insignificant in determining the nucleation and growth of dislocated islands during heteroepitaxy by MBE.

DOI: 10.1103/PhysRevB.68.161304

PACS number(s): 68.55.-a, 61.43.Hv, 81.15.Hi

Crystal growth by epitaxial methods such as molecular-beam epitaxy (MBE) has been a subject of intensive interest because of the quest of artificially structured materials for special device applications. For such materials, the morphology or the smoothness of the surface/interface is of paramount importance. This demands a better understanding of growth mechanisms in order to improve the quality of the film. Recent theoretical efforts have advanced the scaling theory,<sup>1</sup> which describes the size and spatial distributions of islands formed during initial stage growth (submonolayer regime). Specifically, if the system contains only one length scale, i.e., the diffusion-limited average island size  $\langle s \rangle$  or island-island separation  $\langle r \rangle$ , surface areal density of islands,  $N_s(\theta)$ , having the size  $s$  at material coverage  $\theta$  (number of atoms per unit area, or knowing the areal density of epitaxial sites, it can be referred to by the number of layers) is<sup>1</sup>

$$N_s(\theta) = \frac{\theta}{\langle s \rangle^2} f_i(s/\langle s \rangle), \quad (1)$$

where  $f_i(u)$  is the scaling function that depends only on the scaled island size  $u = s/\langle s \rangle$ . Obviously, the density of all islands, irrespective of their sizes, is  $N = \sum N_s$ , and the coverage is  $\theta = \sum s N_s$ . The average island size is then  $\langle s \rangle = (1/N) \sum s N_s$ . The exact form of the scaling function  $f_i(u)$  depends on the critical island size  $i$ , which is the size of the largest unstable island.<sup>1,2</sup> This scaling assumption has been confirmed by computer simulations<sup>1-4</sup> as well as during homoepitaxy of metals<sup>5</sup> and semiconductors.<sup>6</sup> For heteroepitaxial systems such as InAs/GaAs, there are also reports of the scaling behavior in the submonolayer regime<sup>7,8</sup> and also for three-dimensional (3D) islands formed due to the Stranski-Krastanow (SK) growth mode.<sup>9</sup> The latter observations are surprising and indeed unexpected, as it is not obvious why scaling theory applies to a strained system where more than one length scales are present.<sup>7,10,11</sup>

In this Rapid Communication, we report the scaling property of *heteroepitaxial* InN islands formed on GaN(0001) surface during MBE. InN/GaN represents a system with large lattice mismatch ( $\sim 10\%$ ), and the growth follows the

SK mode where 3D islands nucleate after an initial wetting-layer formation.<sup>12</sup> The difference between this system and InAs/GaAs is that the InN islands are dislocated<sup>12,13</sup> whereas they are coherent for InAs.<sup>7-9</sup> The residual strain in InN islands depends on both the size of the islands and the deposition condition (e.g., indium (In) to nitrogen (N) flux ratio).<sup>12</sup> Further, the island shape varies dramatically depending on the condition of MBE.<sup>13</sup> Despite all these variations, the scaling property of both island size and separation distribution is observed. A similar scaling phenomenon has been reported previously for 3D InAs islands,<sup>9</sup> however, there is a key difference between this experiment and that of Ref. 9 in that the 3D InN islands are *dislocated* with the residual strain in islands varies depending on their sizes, whereas for 3D InAs islands, they are coherent having constant strain when they grow.

On a practical note, III-V nitrides represent a family of important material system, which have demonstrated great promise in electronic/optoelectronic applications.<sup>14</sup> InGaN quantum dots (QD's) formed by the SK growth mode can be important ingredients in modern devices, where quantum effects are utilized. The study of InN dot formation is thus of practical importance in the search of incorporating QD's in nitride based devices.

The experiments are conducted in a multichamber ultra-high vacuum (UHV) system, where the MBE reactor and scanning tunneling microscope (STM) are interconnected via UHV interlocks. In MBE, Knudsen cells for gallium (Ga) and In and a plasma unit for N source (Oxford Applied Research, HD-25) are incorporated. The MBE reactor also contains a reflection high-energy electron-diffraction (RHEED) facility allowing real-time surface and strain analyses. Prior to InN deposition, a thick ( $\sim 1 \mu\text{m}$ ) GaN buffer film is grown at  $650^\circ\text{C}$  under a Ga-rich flux condition.<sup>15</sup> The surface is then briefly ( $\sim 1$  min) annealed at the growth temperature before it is dropped to  $370^\circ\text{C}$  for subsequent InN growth. The purpose of the annealing procedure is to remove excess Ga atoms from the buffer film surface, which is known to exist under the MBE conditions employed here. Excess-Ga removal is revealed in RHEED by a pattern

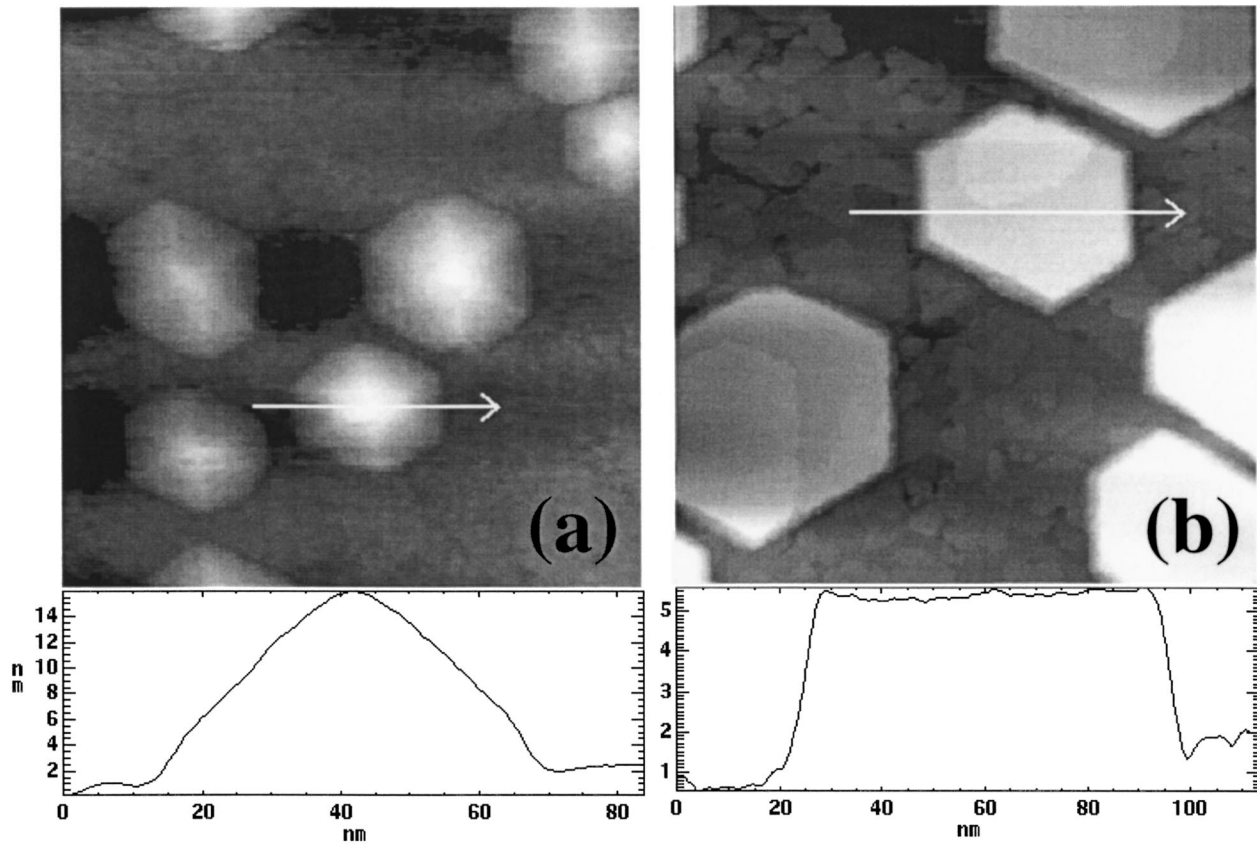


FIG. 1. STM images showing 3D InN islands formed on GaN(0001) following deposition at 370°C under (a) excess-N and (b) excess-In flux conditions. The line profiles reveal the island shapes (note the difference in scale between the two plots). Image size: 200 nm  $\times$  200 nm.

change from pseudo-(1 $\times$ 1) to (2 $\times$ 2).<sup>16</sup> For InN deposition, N flux is fixed at the growth-rate equivalence of 0.033 bilayers (BL's)/s. To investigate the scaling property of 3D InN islands, two sets of samples are grown. In the first set, the In flux less than that of N is chosen (In/N $\sim$ 0.3), while the nominal coverage is varied from 3.3 BL's to 10.9 BL's. For the second set, excess-In flux is adopted (In/N $\sim$ 1.7) and the nominal coverage ranges from 3.3 BL's to 10.1 BL's. Island density measurements as well as STM examination of the surfaces indicate that coalescence occurs for the highest coverages (>9 BL's), which are thus excluded from the scaling analysis. In addition, two more samples are prepared under the In/N flux ratios of  $\sim$ 0.6 and  $\sim$ 1.0, respectively, but for a single and the same nominal coverage of 4.4 BL's. During deposition, the evolution of strain in the film is monitored by RHEED, which shows relaxation before the commencement of 3D islanding.<sup>12</sup> After growth, the sample is thermally quenched. STM imaging of the surface is conducted in an adjacent UHV chamber at room temperature under the constant current mode. The tunneling current is 0.1 nA and the sample bias is  $-2.0$  V for all the STM measurements.

Figure 1 shows surfaces containing 3D InN islands, which are typical for growth under (a) excess-N and (b) excess-In flux conditions. The nominal thicknesses of InN are 8.3 BL's and 6.7 BL's for (a) and (b), respectively. By monitoring the

RHEED,<sup>12</sup> it is found that transition from two-dimensional (2D) wetting layer to 3D islanding takes place at the thickness of 2.9 BL's for the former and 2.3 BL's for the latter cases. The shape of the 3D islands are different between the two (refer to the line profiles in Fig. 1). In the case of using excess-N flux (a), the islands are pyramidal and the sidewalls are seen to be composed of stacks of double bilayer steps, akin to GaN mounds.<sup>17</sup> For islands formed using excess-In flux, they are pillars showing flat tops. This difference in shape is accompanied by distinctly different behavior in aspect ratios of islands as they grow.<sup>13</sup> In general, when excess-In flux is used, the islands show lower aspect ratios than those formed under excess-N condition. Further, with increasing island size, the aspect ratio shows a decreasing trend for both cases, which can be attributed to a gradual relaxation of strain in islands as they grow.<sup>13</sup>

Figure 2 shows the scaled island density for a total of nine sets of data, covering a (nominal) coverage ranging from 3.3 to 8.3 BL's, a growth-rate range from 0.009 to 0.033 BL's/s and also In/N flux ratios between 0.3 and 1.7. The unscaled density curves are given in the inset for only five datasets for clarity. In the figure, each curve represents a distribution of 100–500 islands. Note that in plotting Fig. 2, the coverage  $\theta$  has been calculated according to  $\theta = \sum s_i N_i$ , rather than using the nominal values, as in this way the amount of materials taken by the wetting layer is subtracted. In passing, it is

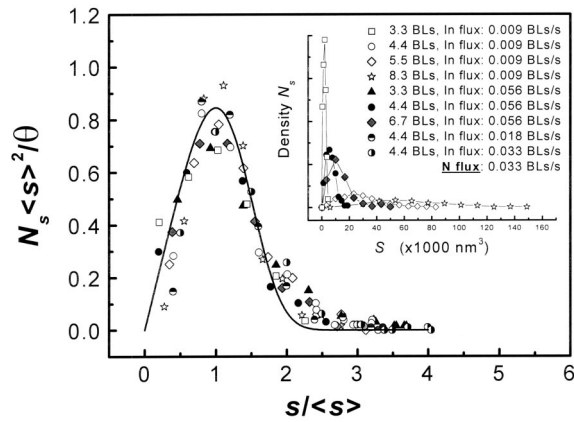


FIG. 2. Scaled density of 3D InN islands (The average volumes range from  $1700 \text{ nm}^3$  to  $65\,000 \text{ nm}^3$ ). The inset shows unscaled densities for five selected datasets, representing different coverages and different deposition conditions. The solid curve in the main plot is the analytic expression of Ref. 2 with critical island size of  $i = 1$ , while the lines in the inset connecting each data point are shown to guide reader's eye.

worth mentioning that materials transfer from the wetting layer to 3D islands upon 2D-3D transition has been noted, which is similar to that of InAs/GaAs(001).<sup>18</sup> In the plot, island size has been referred to by its volume rather than the number of atoms conventionally adopted.<sup>1,2</sup> However, the two are equivalent, having known the atomic density of the material (For InN, it is  $\approx 3.25 \times 10^{22} \text{ cm}^{-3}$ ). In fact, in plotting the scaled quantities, the precise unit one chooses to use is immaterial as long as it is kept consistent. From Fig. 2, it is seen that reasonable collapse of the data is observed, suggesting that the scaling form of Eq. (1) is followed by 3D InN islands. This is despite the variations in island shape and residual strain as noted earlier. Theoretical investigations have predicted that strain can cause a restraint in growth of larger islands<sup>19</sup> and also a preferential size of the islands.<sup>20</sup> If so, scaling of island sizes would not generally follow.<sup>7,10,11</sup> The result of Fig. 2 is thus surprising. It suggests that strain is insignificant in determining the nucleation and growth of 3D InN islands and the system remains diffusion dominant. As noted earlier, strain *does* exist in the islands and is found to be about 1–2% according to RHEED measurements.<sup>12</sup> Thus, it is puzzling why the preferential size is not observed and that the scaling property is unaffected. We believe the explanation may lie in the dislocated nature of the islands. Indeed, because the islands are defected, significant amount of strain is relieved by dislocations. As islands grow, new dislocations are introduced and so more strain is relieved. The continuous relieve of (residual) strain then makes reaching the preferential size of islands unattainable. Large lattice mismatch leads to formation of dislocated islands in general,<sup>21,22</sup> so we expect the scaling behavior to hold in many of such heteroepitaxial systems.

Another observation in Fig. 2 is that the distribution resembles well the one for *homoepitaxial* 2D islands in the submonolayer regime. The solid curve in the figure represents the analytic expression of Amar and Family<sup>2</sup> with the critical island size  $i = 1$ . This is despite the fact that the

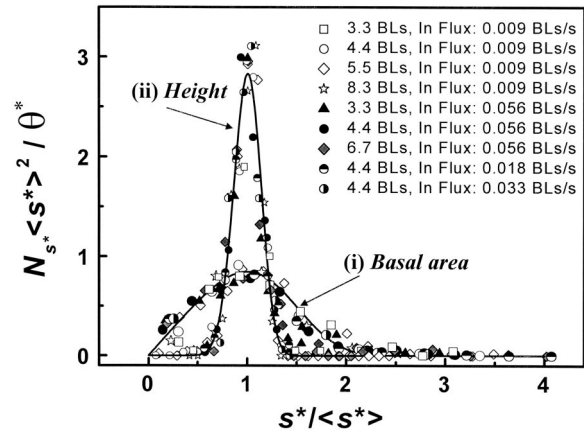


FIG. 3. Scaled density distribution for (i) basal area (average values range from  $650 \text{ nm}^2$  to  $3700 \text{ nm}^2$ ) and (ii) height (average heights range from  $2.6 \text{ nm}$  to  $13.8 \text{ nm}$ ) of the 3D InN islands. The solid curves are analytic expression of Ref. 2, with  $i = 1$  for (i) and  $i = 13$  for (ii).

theory considered no strain in the analyses.<sup>1,2</sup> The critical island size of  $i = 1$  means that only monomers diffuse while dimers or islands with larger sizes do not and are stable. This would imply that no detachment of atoms occurs under the condition employed in this study ( $T = 370^\circ \text{C}$ ). However, as pointed out by Koduvally and Zangwill,<sup>23</sup> if the parameter  $\lambda$  is adopted, which is defined as the ratio between the net detachment rate from an island and the net attachment rate to an island,<sup>24</sup> the above observation may simply reflect that  $\lambda \sim 1$  or less, which can be satisfied even for systems with significant detachment rates.<sup>23</sup>

Since the islands do not have constant aspect ratios,<sup>13</sup> the scaling in size (volume) does not suggest the same for the basal area  $A$  and height  $h$  of the islands. However, as seen in Fig. 3, the two quantities do scale as well. In particular, the basal area follows closely the scaling function of the volume, while the height is much narrowly distributed. The solid curves in the figure are again the theoretical expressions of Ref. 2, with  $i = 1$  and  $i = 13$ , respectively. Note, however, the quantity  $\theta^*$  in these latter two cases do not have the original meaning of being material coverage. Instead, it is merely a measure of the product  $N \langle s^* \rangle$ , where  $N$  is the overall areal density of islands as before, while  $\langle s^* \rangle$  is the average value of the quantity of interest (basal area  $A$  and height  $h$ ). Since island volume is the product of the basal area and height (with different prefactors, depending on island shape), the distribution of the volume is simply a convolution of the distribution functions of the latter two quantities (area and height). The resemblance of the distribution curves between the volume and the basal area is a direct result of the narrow distribution for height. Indeed, had all islands taken the same height (i.e.,  $\delta$ -distribution function), the distributions of volume and basal area would be exactly the same.

Finally, scaling of spatial separation of InN islands is also investigated. According to the scaling assumption, island separation distribution function is<sup>1</sup>

$$\frac{N(r)}{N} = g\left(\frac{r-r_0}{\langle r \rangle}\right), \quad (2)$$

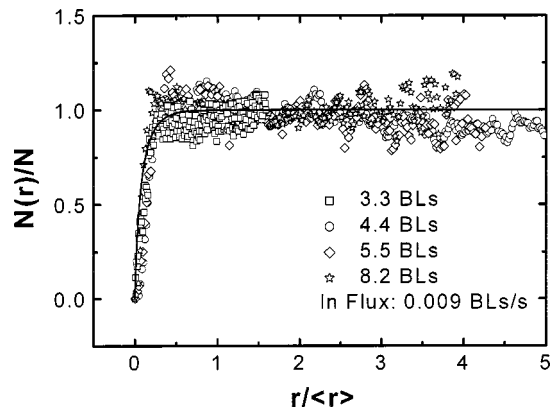


FIG. 4. Scaled pair distribution for 3D InN islands. The solid curve is the analytic expression of Ref. 1 (see text).

which gives the probability of finding an island whose center is a distance  $r$  away from the center of another island. In the equation,  $\langle r \rangle \sim N^{-1/2}$  is a measure of average separation between islands while  $r_0$  is the average radius of islands. The scaling function  $g(\zeta)$  has the property that  $g(0) \rightarrow 0$ , and  $g(\infty) \rightarrow 1$ . Figure 4 shows the collapse of data together with a theoretical curve (solid line) given by  $1 - K_0(\lambda r / \langle r \rangle) / K_0(\lambda r_0 / \langle r \rangle)$ , where  $K_0$  is the modified zero-order Bessel function,<sup>1</sup> and  $\lambda$  is a fitting parameter, which is

$\approx 6$  here. This expression is derived without considering the strain, so the agreement between the experiment and the theoretical curve suggests again that strain is irrelevant in this system. From Fig. 4, one observes no clustering of islands in any azimuthal directions, rather they are randomly distributed on the surface.

To summarize, for the highly strained system of InN on GaN, dislocated 3D islands nucleate under the SK growth mode. Despite variations in strain and shape of the islands, scaling behavior is observed for both island size and spatial distribution. This implies that strain does not play a significant role in determining the nucleation sites and growth of the islands. The cause may lie in the dislocated nature of the islands, so that the constantly decreasing residual strain in islands does not reach the critical strength required to affect the scaling properties of islands. This means that scaling behavior may well be more general than hitherto thought, occurring in many heteroepitaxial systems.

#### ACKNOWLEDGMENTS

We would like to thank W. K. Ho for technical support and C.-H. Lam and D. D. Vvedensky for comments and suggestions. The project was supported by grants from the Research Grants Council of the Hong Kong Special Administrative Region, China (Project Nos. HKU7118/02P and CityU1238/02P).

\*Corresponding author. Email address: mhxie@hkusua.hku.hk

<sup>1</sup>M.C. Bartelt and J.W. Evans, Phys. Rev. B **46**, 12 675 (1992); J.W. Evans and M.C. Bartelt, Surf. Sci. **284**, L437 (1993); M.C. Bartelt, M.C. Tringides, and J.W. Evans, Phys. Rev. B **47**, 13 891 (1993).

<sup>2</sup>J.G. Amar and F. Family, Phys. Rev. Lett. **74**, 2066 (1995).

<sup>3</sup>G.S. Bales and D.C. Chrzan, Phys. Rev. B **50**, 6057 (1994).

<sup>4</sup>C. Ratsch, A. Zangwill, P. Šmilauer, and D.D. Vvedensky, Phys. Rev. Lett. **72**, 3194 (1994).

<sup>5</sup>J.A. Stroschio and D.T. Pierce, Phys. Rev. B **49**, 8522 (1994).

<sup>6</sup>A.R. Avery, H.T. Dobbs, D.M. Holmes, B.A. Joyce, and D.D. Vvedensky, Phys. Rev. Lett. **79**, 3938 (1997).

<sup>7</sup>V. Bressler-Hill, S. Varma, A. Lorke, B.Z. Nosho, P.M. Petroff, and W.H. Weinberg, Phys. Rev. Lett. **74**, 3209 (1995).

<sup>8</sup>G.R. Bell, T.J. Krzyzewski, P.B. Joyce, and T.S. Jones, Phys. Rev. B **61**, R10 551 (2000).

<sup>9</sup>Y. Ebiko, S. Muto, D. Suzuki, S. Itoh, K. Shiramine, T. Haga, Y. Nakata, and N. Yokoyama, Phys. Rev. Lett. **80**, 2650 (1998); Y. Ebiko, S. Muto, D. Suzuki, S. Itoh, H. Yamakosi, K. Shiramine, T. Haga, K. Unno, and M. Ikeda, Phys. Rev. B **60**, 8234 (1999).

<sup>10</sup>C. Ratsch, A. Zangwill, and P. Šmilauer, Surf. Sci. Lett. **314**, L937 (1994).

<sup>11</sup>D.D. Vvedensky (private communication).

<sup>12</sup>Y.F. Ng, Y.G. Cao, M.H. Xie, X.L. Wang, and S.Y. Tong, Appl. Phys. Lett. **81**, 3960 (2002).

<sup>13</sup>Y.G. Cao, M.H. Xie, Y. Liu, H.S. Wu, and S.Y. Tong

(unpublished).

<sup>14</sup>*Gallium Nitride I*, edited by J.I. Pankove and T. D. Moustakas Semiconductors and Semimetals Vol. 50 (Academic, New York, 1998); *Gallium Nitride II*, edited by J. I. Pankove and T. D. Moustakas, Semiconductors and Semimetals Vol. 57 (Academic, New York, 1999).

<sup>15</sup>S.M. Sean, M.H. Xie, W.K. Zhu, L.X. Zheng, H.S. Wu, and S.Y. Tong, Surf. Sci. **445**, L71 (2000).

<sup>16</sup>A.R. Smith, R.M. Feenstra, D.W. Greve, M.-S. Shin, M. Skowronski, J. Neugebauer, and J.E. Northrup, J. Vac. Sci. Technol. B **16**, 2242 (1998).

<sup>17</sup>M.H. Xie, S.M. Seutter, W.K. Zhu, L.X. Zheng, H.S. Wu, and S.Y. Tong, Phys. Rev. Lett. **82**, 2749 (1999).

<sup>18</sup>B.A. Joyce, J.L. Sudijono, J.G. Belk, H. Yamaguchi, X.M. Zhang, H.T. Dobbs, A. Zangwill, D.D. Vvedensky, and T.S. Jones, Jpn. J. Appl. Phys., Part 1 **36**, 4111 (1997).

<sup>19</sup>C. Ratsch and A. Zangwill, Appl. Phys. Lett. **63**, 2348 (1993); C. Ratsch, P. Šmilauer, D.D. Vvedensky, and A. Zangwill, J. Phys. I (France) **6**, 575 (1996).

<sup>20</sup>V.A. Shchukin and D. Bimberg, Rev. Mod. Phys. **71**, 1125 (1999).

<sup>21</sup>J.W. Matthews, D.C. Jackson, and A. Chambers, Thin Solid Films **26**, 129 (1975).

<sup>22</sup>C. Ratsch and A. Zangwill, Surf. Sci. **293**, 123 (1993).

<sup>23</sup>H.M. Koduvely and A. Zangwill, Phys. Rev. B **60**, R2204 (1999).

<sup>24</sup>M.C. Bartelt, L.S. Perkins, and J.W. Evans, Surf. Sci. **344**, L1193 (1995).